ARTICLE

OBC
www.rsc.org/obc

Substituent effects on the ionization reaction of β-mesylate phenethyl radicals †

Sandy F. Lancelot, Frances L. Cozens * and Norman P. Schepp
Department of Chemistry, Dalhousie University, Halifax, Nova Scotia, Canada B3H 4J3. E-mail: fcozens@dal.ca

Received 19th February 2003, Accepted 14th April 2003
First published as an Advance Article on the web 8th May 2003

A series of β-methanesulfonate phenethyl radicals bearing a range of electron donating and withdrawing aromatic substituents were generated and studied in a variety of solvent mixtures using nanosecond laser flash photolysis. Rate constants for the formation of the corresponding styrene radical cation *via* heterolytic loss of the β-mesylate leaving group were measured using time-resolved absorption spectroscopy. The ionization reaction was investigated in a variety of solvents and solvent mixtures including 1,1,1,3,3,3-hexafluoro-2-propanol, 2,2,2-trifluoroethanol, acetonitrile, methanol and water. The influence of substituent electronic effect and solvent polarity on the kinetics of the β-heterolysis reaction are discussed and assessed using the σ^+ Hammett parameter and Y_{OMs} values, respectively. The small magnitude of *m* calculated for the formation of the 4-methoxystyrene radical cation by ionization of the mesylate group ($m = 0.33$) in aqueous methanol mixtures is compared to values obtained for the formation of the same radical cation *via* loss of chloride and bromide where $m = 0.56$ and $m = 0.45$, respectively.

Introduction

An important driving force behind much of the current research into the chemistry of organic free radicals is the recognition that these reactive intermediates can play key roles in biological events.[1–5] One type of radical formed in biological systems that has attracted considerable attention is radicals with a leaving group attached to the carbon adjacent (β) to the radical center.[6] More specifically, the ionization of these radicals through heterolytic loss of the β-leaving group to form an alkene radical cation, eqn. (1), has been linked to reactions catalyzed by enzymes such as diol dehydrase,[4,5,7–12] ethanolamine deaminase,[1,13] and ribonucleotide reductase.[4,5,14–18]

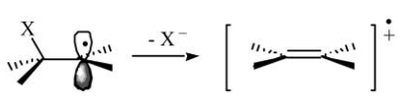

(1)

This kind of reaction has also been proposed as a key step in radiation induced damage to DNA. Following C4′-hydrogen abstraction invoked by radiolytically generated radicals, the resulting 4′-deoxyribosyl radical has a propensity towards phosphate elimination at the β-position (C3′) to the radical center, the culmination of which is scission of the nucleic acid strand,[19–28] eqn. (2).

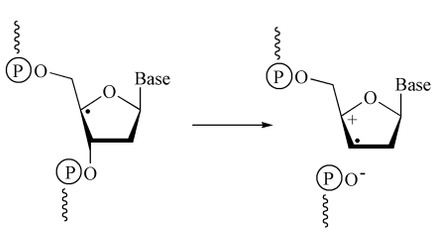

(2)

In an effort to understand how these ionization reactions are influenced by common variables such as the ionizing ability of solvent and leaving group ability, we recently examined the β-heterolysis of bromide and chloride from 4-methoxyphenethyl radicals, Scheme 1.[29] These substrates proved to be ideal since generation of the radical cation upon ionization of the halide from the radical is easily followed using time-resolved nanosecond laser techniques.

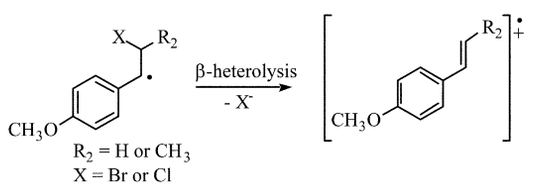

Scheme 1

Our results also showed that no ionization occurred when the 4-methoxy group was replaced by a less electron-donating group like 4-methyl or hydrogen. This result strongly suggested a significant substituent effect on the dynamics of the β-heterolysis reaction.[30] However, since no rate constants could be measured for the 4-methyl or the unsubstituted derivatives, no quantitative measure of the substituent effect could be determined. In the present work, we report on results obtained using mesylate ($CH_3O_2SO^-$) at the β-position of the aryl substituted phenethyl radicals **2a**–**e** generated upon laser irradiation of precursors **1a**–**e**, Scheme 2. Since mesylate is an effective leaving group in these reactions,[21,31,32] ionization of the radicals to the corresponding radical cations **3a**–**e** was observed for a wide range of aryl substituents, thus allowing a quantitative measure of the effect of aryl substituents on the rate constant for the β-heterolysis reaction.

Results

Laser photolysis in acetonitrile

Laser flash photolysis using 266 nm excitation of 2-(4-chlorophenyl)-3-oxobutyl methanesulfonate **1a** in nitrogen-saturated acetonitrile (MeCN) leads to the transient absorption spectrum shown in Fig. 1a. The spectrum shows a transient species with strong absorption at 280 nm. Monitoring the change in optical density (ΔOD) as a function of time at this wavelength gives a decay trace that fits nicely to second-order kinetics with a calculated decay rate constant $2k/\varepsilon l = 3.1 \times 10^5\ s^{-1}$. The transient species is relatively long-lived under nitrogen-saturated

† Electronic supplementary information (ESI) available: Tables of rate constants and Hammett substituent parameters for ionization of radicals **1a**–**e** in various solvent mixtures. See http://www.rsc.org/suppdata/ob/b3/b301959d/

DOI: 10.1039/b301959d

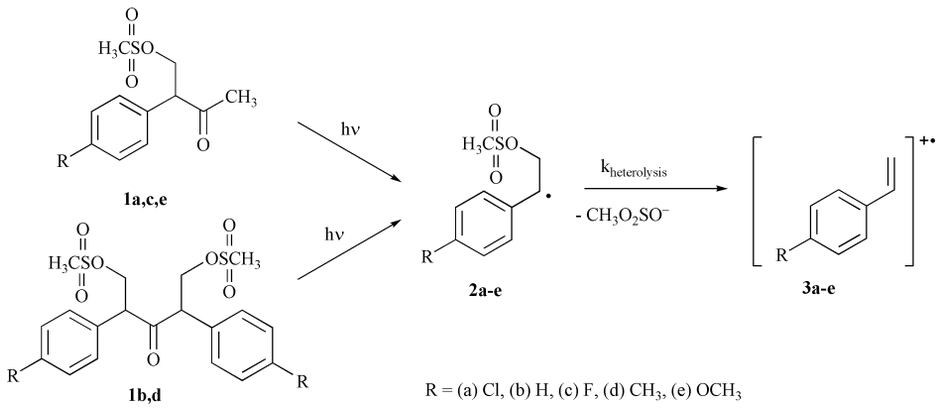

Scheme 2

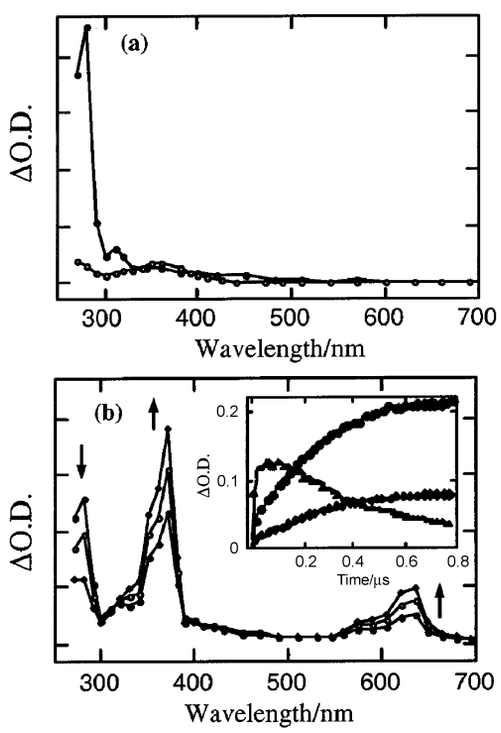

Fig. 1 a) Transient absorption spectra obtained 0.21 μs after 266 nm laser irradiation of 2-(4-chlorophenyl)-3-oxobutyl methanesulfonate **1a** in (●) nitrogen- and (○) oxygen-saturated MeCN. b) Transient absorption spectra (●) 0.07 μs, (○) 0.2 μs, and (◆) 0.6 μs after irradiation of **1a** in nitrogen-saturated 70% HFIP–30% TFE. The inset shows the time-resolved absorption changes at (△) 280 nm, (●) 370 nm and (◆) 630 nm.

conditions but is completely quenched by the addition of oxygen, a known potent radical scavenger, to the solution, Fig. 1a. The second-order decay process under nitrogen conditions combined with the rapid oxygen quenching and location of the absorption maximum near 300 nm[33] is consistent with the identification of the transient species as the β-methanesulfonate 4-chlorophenethyl radical **2a** produced by α-cleavage of the C–$COCH_3$ bond of precursor **1a**, eqn. (3).

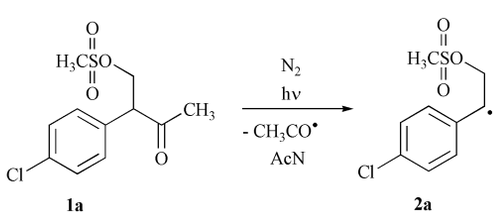

(3)

Similar results were observed upon laser irradiation of precursors **1b**–**e**, Scheme 2, in acetonitrile. In each case, a single transient species with an absorption maximum in the 280–300 nm range was observed and assigned to the β-methanesulfonate arylethyl radical **2b**–**e**. In addition, the radicals in all cases were fully formed within the laser pulse. While such rapid formation is expected for radicals **2a**,**c**, and **e**, which are produced exclusively by excited state α-cleavage, the symmetrical substituted diaryl acetone precursors **1b** and **1d** produce radicals **2b** and **2d**, respectively, by decarbonylation of an acyl radical, as well as by α-cleavage of the excited precursor, eqn. (4). However, the decarbonylation reaction of the methylphenylacyl radical is known to occur rapidly with a rate constant of *ca.* 5×10^7 s^{-1}.[34] In addition, due to the influence of the 4-methyl group on the reaction rate constant, decarbonylation to produce radical **2d** is likely to occur with a slightly larger rate constant.[35] Thus, prompt formation of radicals **2b** and **2d** is also consistent with expectation and, more importantly, indicates that the time-resolved processes occurring after the laser pulse as described below represent reactions of the fully formed radicals and are, in general, not influenced by the presence of the decarbonylation step.

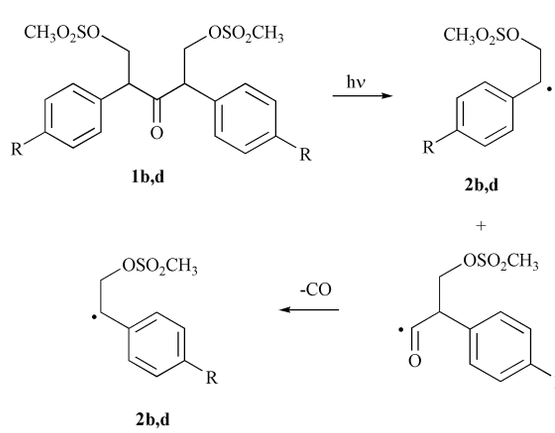

(4)

Laser photolysis in HFIP–TFE mixtures

In nitrogen-saturated 1,1,1,3,3,3-hexafluoro-2-propanol (HFIP), laser flash photolysis of **1a** again generates the β-methanesulfonate 4-chlorophenethyl radical **2a** with absorption at 280 nm, but this band now decays in a first-order manner, Fig. 1b. More importantly, concurrent with the decay at 280 nm is a first-order growth in absorption at 370 and 630 nm. The end ΔOD at 370 nm is approximately three times the intensity of the band centered at 630 nm. The location of the observed absorption maxima at 370 and 630 nm, in addition to their relative intensities, reveals that the transient responsible for these signals is the 4-chlorostyrene radical cation **3a**, formed *via* heterolytic loss of the β-mesylate group, eqn. (5) (R = 4-chloro).

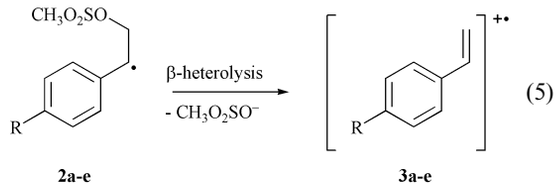

(5)

2a-e **3a-e**

Consistent with the generation of radical cation **3a** from radical **2a** *via* β-heterolysis of the mesylate group is the identical rate constant of 1.3×10^6 s^{-1} for the first-order formation of the 370 and 630 nm absorption bands and the decay of the radical at 280 nm, Fig. 2 inset. In HFIP the 4-chlorostyrene radical cation was found to be relatively long-lived with a decay rate constant $k = 2.0 \times 10^5$ s^{-1} and was rapidly quenched *via* the introduction of a good nucleophile such as Br^- to the solution, as expected for a cationic transient species.

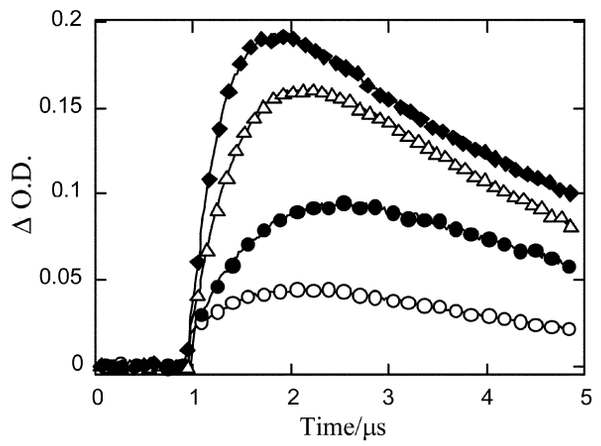

Fig. 2 Time-resolved growth at 630 nm observed upon 266 nm laser irradiation of 2-(4-chlorophenyl)-3-oxobutyl methanesulfonate **1a** in nitrogen-saturated HFIP–TFE mixtures containing (○) 40%, (●) 60%, (△) 80%, and 100% HFIP (◆).

Results obtained in oxygenated HFIP provide further evidence that ionization of radical **2a** is indeed the mechanism by which radical cation **3a** is produced. As anticipated, oxygen causes the complete disappearance of the 280 nm absorption band due to rapid trapping of radical **2a** by oxygen. In addition, the two characteristic absorption bands at 370 and 630 nm associated with the 4-chlorostyrene radical cation **3a** are also largely quenched by the introduction of oxygen to the solution. Since oxygen is not known to react rapidly with styrene-type radical cations,[36] it is unlikely that the disappearance of the radical cation is due to its direct interaction with oxygen. However, the results obtained in neat MeCN and HFIP are in agreement with a mechanism involving the β-heterolysis reaction, in which radical formation directly precedes that of radical cation formation. Therefore, following the photogeneration of β-substituted radical **2a** in a nitrogen-saturated polar solvent such as HFIP, ionization of the mesylate group yields radical cation **3a**. However, oxygen inhibits the β-heterolysis process by providing radical **2a** with an alternative decay route against which the kinetics of the β-heterolysis reaction cannot compete.[29] Thus, under such conditions, the direct product of the β-heterolysis reaction, the radical cation, is not observed.

The fact that the 4-chlorostyrene radical cation is not observed in MeCN yet is successfully generated in HFIP infers that its formation is heavily dependent on the nature of the solvent. To investigate this further, experiments were carried out in a series of HFIP–2,2,2-trifluoroethanol (TFE) solvent mixtures. Several representative kinetic traces attained at 630 nm for the formation of the 4-chlorostyrene radical cation **3a** are given in Fig. 2. As shown, they highlight a distinct correlation between HFIP content and absorption intensity, a value that is proportional to the concentration of the radical cation. These solvent effects are quantified with the corresponding kinetics where in neat HFIP the measured rate constant $k = 3.0 \times 10^6$ s^{-1} is approximately three times faster than that obtained in a solution of 50% HFIP–50% TFE where $k = 9.2 \times 10^5$ s^{-1}. Accurate rate constants could not be obtained in mixtures containing less than 50% HFIP, due to minimal change in optical density at 630 nm.

Precursors **1b**–**e**, Scheme 2, were also subjected to laser photolysis experiments in HFIP–TFE mixtures. In each case the formation of the corresponding styrene-type radical cation **3b**–**e** from the photogenerated radicals **2b**–**e** was clearly evident *via* the transient absorption spectra that revealed strong absorption in the 360 and 600 nm region. The time-resolved growth kinetics for the β-heterolysis reaction were measured in each case in varying HFIP content in TFE, except for the 4-methoxy radical **2e** whose reaction could only be resolved in neat TFE. The rate constants acquired in HFIP–TFE mixtures for the reactions of **2a**–**e** are summarized in Fig. 3.

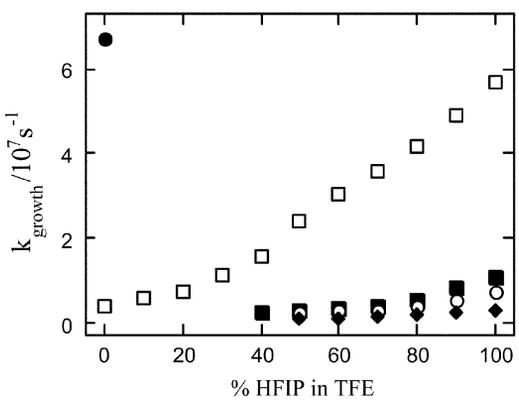

Fig. 3 Rate constants for the growth of the (●) 4-methoxy, (□) 4-methyl, (■) 4-fluoro, (○) unsubstituted, and (◆) 4-chlorostyrene radical cation measured between 600–630 nm as a function of HFIP % (v/v) in TFE, following 266 nm laser flash photolysis of the corresponding precursors under nitrogen-saturated conditions.

Radicals **2a**, **2c** and **2e** were all generated rapidly within the laser pulse by α-cleavage, so the rate constants for ionization given in Fig. 3 were all unaffected by the rate constant for the formation of the radical. This was true even for β-heterolysis of the 4-methoxy derivative **2e**, which occurred with a very fast rate constant of $k = 6.7 \times 10^7$ s^{-1} in neat TFE. However, as mentioned earlier, radicals **2b** and **2d** are generated by slower decarbonylation as well as by fast α-cleavage, and the possibility exists that decarbonylation may be a limiting factor in the kinetics for the formation of radical cations **3b** and **3d**. However, the fastest rate constant measured for ionization of mesylate from radical **2b** was 7.5×10^6 s^{-1}, which is almost one order of magnitude slower than the rate constant for decarbonylation of the similar methylphenylacyl radical.[34] Thus, the ionization rate constants for **2b** cannot be influenced by the decarbonylation reaction. The rate constants for formation of the radical cation from the 4-methyl derivative **2d** were also all significantly slower than decarbonylation, except for that measured in neat HFIP where $k = 5.7 \times 10^7$ s^{-1}. In this case, decarbonylation and ionization may be occurring with similar rate constants. The possibility that, in this solvent, the rate constant for ionization of **2d** might be greater than that for decarbonylation was considered. However, if so, biphasic kinetics would have been observed, with radical cation formation by loss of mesylate from the radical generated by initial α-cleavage occurring promptly within the laser pulse, followed by a time-resolved growth of the radical cation by rate-limiting decarbonylation. Such biphasic kinetics were not observed, and we can conclude that the growth of the radical cation in neat HFIP

represents a good estimate of the rate constant for ionization under these conditions.

It can be noted that solvent effects on the β-heterolysis reaction are exhibited with each precursor **1a**–**d** although clearly not to the same degree. The 4-methyl substituted radical **2d** exhibited the largest solvent effect, with its rate constant for β-heterolysis rising from $k = 4.1 \times 10^6$ s^{-1} in neat TFE to a value approximately fourteen times faster in neat HFIP where $k = 5.7 \times 10^7$ s^{-1}. It is equally apparent from Fig. 3 that the nature of the substituent has a significant impact on the rate constant for the ionization of the mesylate group from these β-substituted radicals. For example in neat HFIP, the rate constant of β-heterolysis obtained when the aromatic substituent R is a 4-methyl group, $k = 5.7 \times 10^7$ s^{-1}, is approximately 19 times faster than with the 4-chloro substituent where $k = 3.0 \times 10^6$ s^{-1}. Such electronic influences also affect the TFE–HFIP solvent composition in which the β-heterolysis reaction is energetically favorable. For instance when R = 4-methyl, the growth of the radical cation *via* β-heterolysis is measurable between 100% TFE and 100% HFIP. In contrast, when R = 4-chloro, formation of the corresponding radical cation is limited to TFE solutions containing 50 to 100% HFIP, *i.e.* more polar solution mixtures.

β-Heterolysis of radicals 2a–e in HFIP–MeCN mixtures

Precursors **1a**–**e** were photolyzed in HFIP–MeCN solvent mixtures and the resulting kinetic data for the β-heterolysis of the mesylate group are presented in Fig. 4. From the data it is again clear that the solvent ionizing ability and the aromatic substituent play key roles in influencing the rate constant for the β-heterolysis reaction. The solvent composition where the β-heterolysis reaction was observed ranged from between 10 and 70% HFIP in MeCN for the 4-methoxy derivative **2e** and 94.5 and 100% HFIP for the 4-chloro **2a** derivative. For the 4-methoxy case the measured rate constant is seen to increase rapidly in MeCN solutions with greater than 40% HFIP, from 4.4×10^6 s^{-1} in 50% HFIP to 5.7×10^7 s^{-1} in 70% HFIP. Also noteworthy, is that the resulting radical cation **3e** is detected in mixtures of much lower polarity relative to the 4-chloro radical **2a**. In solutions containing greater than 70% HFIP the rate constants for the growth of the 4-methoxystyrene radical cation **3e** were too fast to be measured successfully. From the data in Fig. 4 it is clear that even for the 4-fluoro and 4-methyl derivatives the solvent range is significantly reduced compared to the 4-methoxy case. The small solvent range for the 4-chloro and the unsubstituted derivatives clearly indicate the strong dependence of the reaction on the ionizing ability of the solvent and the important contribution from the aromatic substituent to help stabilize the transition state for the ionization reaction.

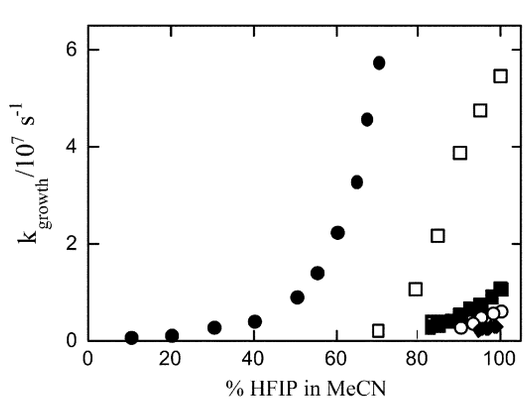

Fig. 4 Rate constants for the growth of the (●) 4-methoxy, (□) 4-methyl, (■) 4-fluoro, (○) unsubstituted, and (◆) 4-chlorostyrene radical cation measured between 600–630 nm as a function of HFIP % (v/v) in MeCN, following 266 nm laser flash photolysis of the corresponding precursors under nitrogen-saturated conditions.

β-Heterolysis of 2e in varying solvent mixtures

In TFE–MeCN solvent mixtures that are inherently less polar, ionization of the β-methanesulfonate 4-methoxyphenethyl radical **2e** is readily detected in solutions containing 20–100% TFE. Fig. 5 is a representative spectrum obtained from these experiments. The decay of the 300 nm absorption band of radical **2e** is clearly seen to be concurrent with the growth of the 350 and 590 nm absorption bands, the known absorption maxima of the 4-methoxystyrene radical cation.[36] An isosbestic point is apparent around 320 nm, a further indication that the rate constant for the decay of radical **2e** parallels that of the rate constant for the growth of radical cation **3e**.

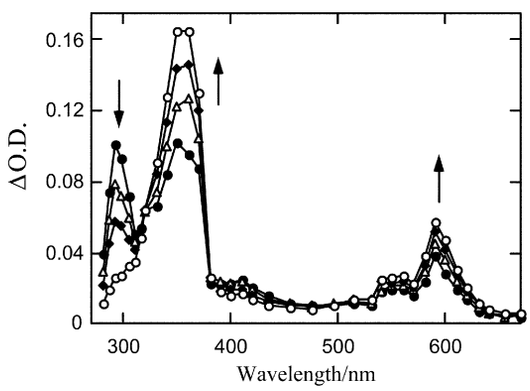

Fig. 5 Absorption spectra after 266 nm laser irradiation 2-(4-methoxyphenyl)-3-oxobutyl methanesulfonate **1e** in 50% TFE–50% MeCN. Spectra were recorded (●) 80 ns, (△) 170 ns, (◆) 280 ns, and (○) 670 ns after the laser pulse.

Further solvent effects for the formation of the 4-methoxystyrene radical cation are clearly shown in Fig. 6 where the rate constants measured in MeCN mixtures with TFE and water as co-solvents and in methanol with water as the co-solvent are presented. As expected, the trend observed is based on solvent polarity, *i.e.* rate constants for ionization decrease with increasing MeCN or methanol content. However, from this data it is clear that methanol is more favorable for ionization of the mesylate group than MeCN. In mixtures containing 40% water, time-resolved growth of the radical cation **3e** was observed with a rate constant of $k = 8.8 \times 10^6$ s^{-1} with MeCN as the co-solvent and $k = 3.7 \times 10^7$ s^{-1} with methanol as the co-solvent, approximately five times faster.

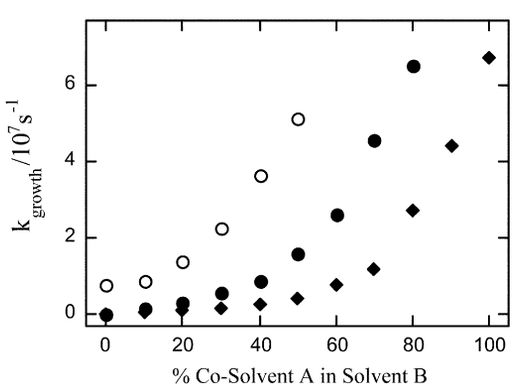

Fig. 6 Growth of the 4-methoxystyrene radical cation **3e** measured at 590 nm upon 266 nm irradiation of 2-(4-methoxyphenyl)-3-oxobutyl methanesulfonate **1e** as a function of co-solvent A (◆) % TFE and (●) % water in nitrogen-saturated MeCN (B) and as a function of co-solvent A (○) % water in nitrogen-purged methanol (B).

Discussion

Substituent effects

The results obtained in this work clearly show that a strong connection exists between the nature of the aromatic substit-

uent and the magnitude of the rate constants measured for the ionization of the β-mesylate phenethyl radicals. For example, in neat TFE, the 4-methoxy derivative **2e** undergoes ionization of the β-mesylate group with a rate constant that is 15-fold greater than the rate constant for the same reaction of the 4-methyl derivative **2d**. In addition, the 4-methyl derivative **2d** has an ionization rate constant that is 5 times faster than the 4-fluoro derivative **2c** under identical solvent conditions of neat HFIP, Fig. 3.

A more quantitative measure of the substituent effects can be obtained from the Hammett correlations presented in Fig. 7, where the rate constants measured for the generation of the styrene-type radical cations **3a**–**d** in varying HFIP–TFE solvent mixtures are plotted against σ^+ parameters. These correlations include results from rate constants for ionization of mesylate from the 4-Me, 4-F, 4-H and 4-Cl derivatives. Results from the 4-MeO derivative are excluded since its reactivity was too fast to measure in solvents in which rate constants for the other derivatives were sufficiently slow to measure.

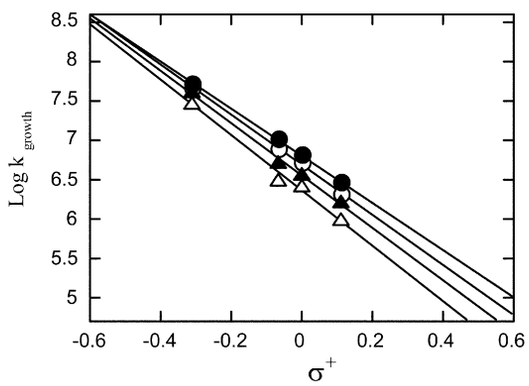

Fig. 7 Hammett plots of the log of the observed rate constants for the growth of the various 4-chloro, unsubstituted, 4-fluoro, and 4-methylstyrene radical cations as a function of σ^+ values in nitrogen-purged (●) neat HFIP, (○) 90% HFIP–10% TFE, (▲) 80% HFIP–20% TFE, and (△) 70% HFIP–30% TFE.

Excellent correlations ($r^2 > 0.99$) are seen in each solvent mixture, with negative slopes giving sensitivity parameters from $\rho^+ = -3.0$ to -3.5. On the other hand, poor correlations ($r^2 < 0.89$) are observed when σ parameters are used instead of σ^+ parameters. The better correlation with σ^+ values is consistent with a situation where the positive charge is delocalized by a resonance interaction between the aromatic ring and the developing positive charge, with the radical center acting as a mediator, Scheme 3.

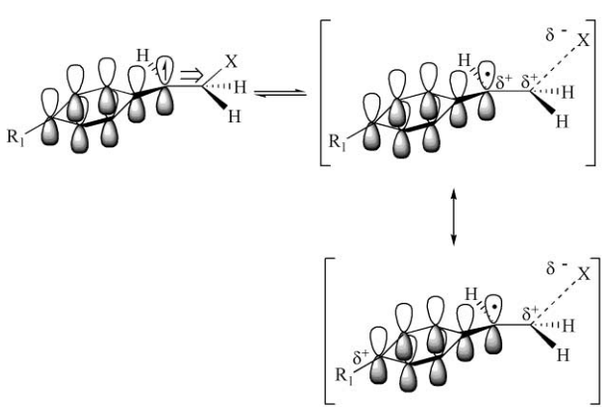

Scheme 3

The $\rho^+ \approx -3$ measured in the present work represents a substantial substituent effect, but even larger effects are observed for S_N1 reactions of benzylic derivatives; for example, the ρ^+ value for the solvolysis of substituted benzyl tosylates in TFE is near -4.5.[37] The lower value for the ionization reaction of the β-substituted phenethyl radicals may reflect an inability of the radical center to fully transmit the electron-donating or electron-withdrawing ability of the aryl substituent. This is similar to reduced substituent effects observed upon insertion of a vinyl moiety between a reaction center and the substituted ring.[38] More important, however, is the enormous difference in reactivity of the β-mesylate arylethyl radicals compared to arylmethyl mesylates, Scheme 4. For example, the rate constant of 2×10^7 s^{-1} for ionization of mesylate from the 4-methoxyphenethyl radical **2e** in 20% aqueous methanol measured in the present work is over 1×10^6 fold greater than the rate constant of 6.1 s^{-1} for ionization of mesylate from 4-methoxybenzyl mesylate in 20% aqueous ethanol at 25 °C.[39] Similarly, ionization of mesylate from the unsubstituted phenethyl radical **2c** in HFIP is 5×10^7 fold more rapid than ionization of mesylate from benzyl mesylate in the same solvent.[40] The large magnitude of the rate constants for the reaction of the arylethyl radicals most likely reflects a transition state that appears much earlier along the reaction pathway as compared to the closed shell benzyl mesylates. In this earlier transition state, charge formation is less developed, and the ability of the aryl substituents to influence the stability of the transition state is considerably weakened.

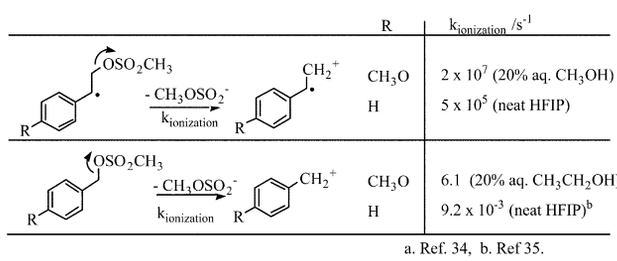

Scheme 4

Sensitivity parameters ρ^+ as a function of solvent composition for the HFIP–TFE mixtures studied are presented in Fig. 8. In each case, the magnitude of ρ^+ is relatively large with values ranging from $\rho^+ = -3$ to -3.5 illustrating a moderately high sensitivity to electronic effects. Interestingly, Fig. 8 reveals that the degree of sensitivity to these electronic effects decreases as the solvent composition becomes less polar. In 60% HFIP–40% TFE, we observe the greatest sensitivity toward substituent effects with a value of $\rho^+ = -3.5$. As the HFIP content is increased to 100%, the magnitude of ρ^+ decreased by 0.5 to a value of $\rho^+ = -3.0$. Two kinetically relevant effects account for the results shown in Fig. 8, electronic and solvent effects. The data reveal that under the highly ionizing conditions offered by neat HFIP, the solvation energy provided by the solvent reduces the electronic requirements, and leads to a smaller absolute value of ρ^+. Further-

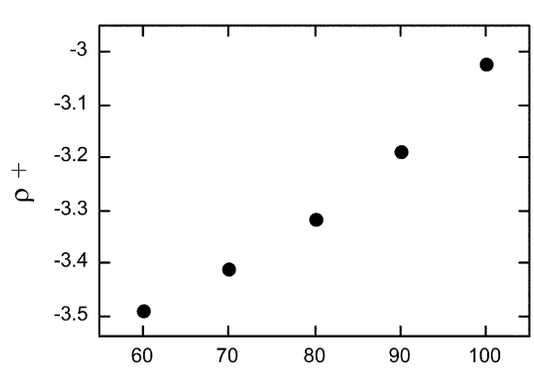

Fig. 8 Slopes (ρ^+) of the Hammett plots as a function of % HFIP in TFE (v/v).

more, as the % content of HFIP is decreased and that of TFE increased, the sensitivity of the reaction to the electronic nature of the aromatic substituent gains greater significance. This seems fitting since the reaction conditions are now less polar and hence less able to stabilize charge formation in the transition state.

Effect of leaving group and solvent

As shown in Fig. 9, the rate constants acquired for the loss of mesylate from the β-mesylate 4-methoxyphenethyl radical **2e** in aqueous methanol are always faster than those measured for the β-bromo and β-chloro compounds studied previously under identical experimental conditions.[29] This is consistent with the well-known enhanced leaving group ability of mesylate compared to the halides. However, the rate constant for ionization of mesylate is only about six fold greater than that for ionization of chloride, a rate enhancement that is considerably smaller than that typically observed in more conventional S_N1 reactions. For example, the rate constant of 0.01 s^{-1} for ionization of bromide from 4-methoxybenzyl bromide in 20% aqueous ethanol is 600 times smaller than the rate constant for loss of mesylate from 4-methoxybenzyl mesylate under similar conditions.[41]

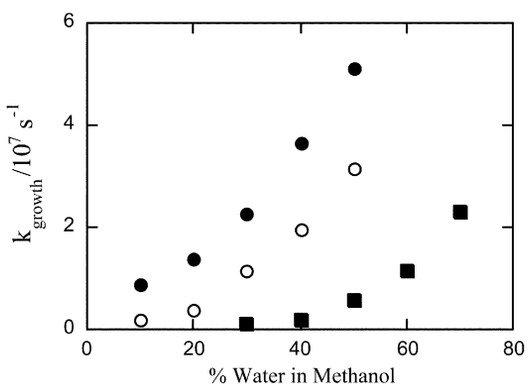

Fig. 9 Rate constant for the growth of the 4-methoxystyrene radical cation **3e** measured at 590 nm upon 266 nm irradiation of 2-(4-methoxyphenyl)-3-oxobutyl methanesulfonate (●), 1-acetoxy-2-bromo-1-(4-methoxyphenyl)ethane (○), and 1-acetoxy-2-chloro-1-(4-methoxyphenyl)ethane (■) as a function of water content (% v/v) in nitrogen-saturated methanol. Data for (○) and (■) were taken from reference 29.

The decreased sensitivity to leaving group ability is likely due to an early transition state in which the leaving group–carbon bond is still largely intact. Factors which control the leaving group ability are therefore incompletely felt, and the overall sensitivity of the reaction to the leaving group is diminished.

Larger leaving group effects are observed for the 4-methyl and 4-hydrogen radicals. For example, in 100% HFIP, the β-mesylate 4-methylphenethyl radical **2d** undergoes loss of the mesylate anion with a rate constant of $5.7 \times 10^7\ s^{-1}$, while the corresponding β-bromo and β-chloro radicals do not undergo detectable amounts of β-heterolysis under the same experimental conditions. The rate constants for the loss of bromide and chloride are therefore less than $10^5\ s^{-1}$, indicating at least a 500 fold decrease in the rate constant upon going from the β-mesylate derivative to the β-halide derivatives. The effect of solvent is also less dramatic than expected for a reaction involving ionization of a leaving group. This is illustrated in the Grunwald–Winstein plot, Fig. 10, which shows the relationship between the rate constant for ionization of β-mesylate derivative in methanol–water mixtures and the corresponding Y_{OMs} values for the methanol–water mixtures. The solvent sensitivity parameter *m* derived from the slope of such plots is typically near 1 for a pure S_N1 reaction, with values less than 1 indicating a high degree of nucleophilic assistance from the solvent. The

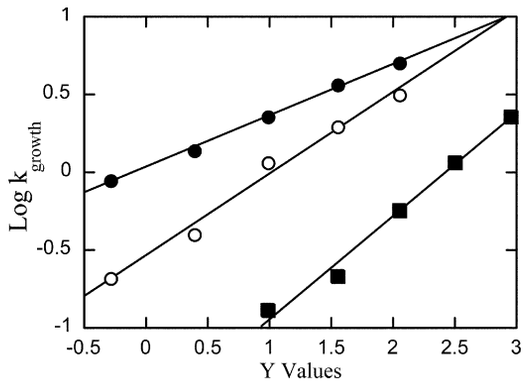

Fig. 10 Relationship between the log of the observed rate constant for the formation of the 4-methoxystyrene radical cation **3e** measured at 590 nm upon 266 nm irradiation of 2-(4-methoxyphenyl)-3-oxobutyl methanesulfonate (●), 1-acetoxy-2-bromo-1-(4-methoxyphenyl)ethane (○), and 1-acetoxy-2-chloro-1-(4-methoxyphenyl)ethane (■) as a function of Y_{OMs}, Y_{Br} and Y_{Cl} values obtained from the solvolysis of the corresponding 2-adamantyl-X substrates. Data for (○) and (■) were taken from reference 29.

relatively low value for the slope, $m = 0.33$, for the reaction of the β-mesylate derivative would therefore ordinarily be interpreted to indicate that the reaction proceeds *via* an S_N2-like transition state, with solvent acting as the incoming nucleophile. However, since the radical cation is always observed as the initial product of the reaction, the loss of mesylate must involve direct cleavage of the mesylate–carbon bond, with little if any direct nucleophilic assistance from the solvent. Instead, the low *m* value is once again more likely a consequence of the high reactivity of the radical toward loss of mesylate. The reactant-like transition state contains little charge formation, and charge stabilizing solvent effects are minimized. The diminished effect of solvent ionizing ability can also be observed upon comparison of the more reactive β-mesylate radical to the less reactive β-chloride and β-bromide derivatives, Fig. 10. The solvent sensitivity parameters of $m = 0.56$ for Cl^- and $m = 0.45$ for Br^- are still significantly less than 1,[29] as expected for the rapid ionization of these halides. However, the *m* values are considerably greater than the value of $m = 0.33$ for the more reactive mesylate derivative. This is consistent with the better leaving group ability of the highly delocalized mesylate group and the faster rate constants for the β-heterolysis reaction involving the loss of the mesylate as compared to the halide derivatives.

Experimental section

Materials

Acetonitrile used for the kinetics experiments was spectroscopic grade (Omnisolve, BDH). 2,2,2-Trifluoroethanol and 1,1,1,3,3,3-hexafluoro-2-propanol were purchased from Aldrich and used as received. Methanol and water were doubly distilled prior to use.

The precursors 2-(4-chlorophenyl)-3-oxobutyl methanesulfonate **1a**, 2,4-diphenyl-3-oxopentyl 1,5-dimethanesulfonate **1b**, 2-(4-fluorophenyl)-3-oxobutyl methanesulfonate **1c**, 2,4-bis(4-methylphenyl)-3-oxopentyl 1,5-dimethanesulfonate **1d**, and 2-(4-methoxyphenyl)-3-oxobutyl methanesulfonate **1e** were synthesized by mesylation of the corresponding alcohols prepared by base catalyzed formylation of appropriate arylacetones or 1,3-diarylacetones. Four of the five acetone derivatives (4-fluorophenylacetone, 4-methoxyphenylacetone, 1,3-diphenyl-2-propanone and 4-chlorophenylacetone) were commercially available and used as received. 1,3-Bis(4-methylphenyl)-2-propanone was prepared as described earlier[42] using magnesium chloride instead of barium chloride, and purified by recrystallization from ethanol.

The ketones were subsequently converted to the required alcohols in a mixed aldol condensation reaction. Potassium carbonate (0.1 g) was dissolved in 50 mL of absolute ethanol and the solution was left to cool to 0 °C in an ice bath. The dibenzylketone (R = H, 4-CH_3) or phenylacetone (R = 4-OCH_3, 4-Cl, 4-F) derivative was subsequently added (4.5 mmol) and the mixture was left to stir for a further 30 minutes. Formaldehyde (40% aqueous solution; 3 molar equivalents per CH_2OH group added) diluted with 5 mL ethanol was added dropwise with continuous stirring. After 1 to 4 hours, the reaction was quenched by adding cold brine (20 mL) and then extracted three times with diethyl ether (30 mL). The combined organic layers were dried with magnesium sulfate and the solvent removed under reduced pressure. The crude product mixtures were purified by flash column chromatography using ethyl acetate–hexane mixtures, or by cold recrystallization from ethyl acetate–hexane mixtures.

All materials were characterized by ^{1}H- and ^{13}C-NMR (Bruker 250 MHz) using $CDCl_3$ as the solvent.

3-(4-Fluorophenyl)-4-hydroxy-2-butanone

Pale yellow oil, enantiomeric mixture; ^{1}H NMR δ 2.07 (1H, s), 2.66 (1H, broad peak), 3.62–3.71 (1H, m), 3.84–3.96 (1H, m), 4.03–4.13 (1H, m), 7.01–7.19 (4H, AA′BB′ pattern); ^{13}C NMR δ 29.61, 60.68, 63.94, 116.01, 116.36, 130.14, 130.28, 131.41, 131.47, 162.46 (d, J = 248.0 Hz), 209.00; UV (CH_3CN) λ_{max} (nm) 264 (1.80), 270 (1.61); EIMS m/z (%) 182 ($M^{\bullet+}$, 0.6), 139 (3), 123 (6), 122 (100), 121 (4), 109 (7), 42 (20); HRMS: found 182.0742 (±0.0008) u, calculated 182.0743 u for $C_{10}H_{11}FO_2$.

3-(4-Methoxyphenyl)-4-hydroxy-2-butanone

Fine white powder, enantiomeric mixture; mp 50–51 °C; ^{1}H NMR δ 2.08 (3H, s), 2.32 (1H, dd, J = 5.50, 7.93 Hz), 3.62–3.72 (1H, m), 3.79 (3H, s), 3.80–3.86 (1H, m), 4.05–4.15 (1H, m), 6.86–7.13 (4H, AA′BB′ system); ^{13}C NMR δ 29.53, 55.42, 60.83, 64.18, 114.75, 127.62, 129.74, 159.40, 209.67; UV (CH_3CN) λ_{max} (nm) 277 (1.53), shoulder at 283 (1.33); EIMS m/z (%) 194 ($M^{\bullet+}$, 16), 151 (86), 134 (79), 133 (72), 121 (100), 119 (36), 91 (91), 77 (45); HRMS: found 194.0945 (± 0.0008) u, calculated 194.0943 u for $C_{11}H_{14}O_3$.

3-(4-Chlorophenyl)-4-hydroxy-2-butanone

Pale yellow oil; ^{1}H NMR δ 2.07 (3H, s), 3.62–3.71 (1H, m), 3.80–3.85 (1H, m), 4.02–4.16 (1H, m), 7.04–7.36 (4H, AA′BB′ system); ^{13}C NMR δ 29.72, 58.6, 63.8, 129.7, 130.2, 133.4, 134.3, 209.8; UV (CH_3CN) λ_{max} (nm) 267 (0.45), shoulder at 275 (0.37), 296 (0.28); EIMS m/z (%) 198 ($M^{\bullet+}$, 0.6), 155 (43), 140 (18), 138 (100), 125 (17), 35 (16); HRMS: found 198.0482 (± 0.0008) u, calculated 198.0476 u for $C_{10}H_{11}O_2Cl$.

2,4-Bis(4-methylphenyl)-1,5-dihydroxy-3-pentanone

Fine colorless needles, diastereomeric mixture; mp 92–93 °C; ^{1}H NMR δ 1.99 (1H, dd, J = 6.10, 7.63 Hz), 2.11 (1H, dd, J_1 = 6.1 Hz, J_2 = not resolved), 2.28 and 2.35 (6H, s), 3.59–4.20 (6H, m), 6.82–7.19 (8H, two sets of AA′BB′ patterns); ^{13}C NMR δ 21.10, 58.56, 60.99, 63.86, 64.97, 128.72, 129.33, 130.11, 131.89, 137.29, 211.11, 211.78; UV (CH_3CN) λ_{max} (nm) 264 (0.76), 272 (0.66), 292 (0.40); EIMS m/z (%) 298 ($M^{\bullet+}$, 52), 268 (100), 135 (39), 118 (62), 117 (17); HRMS: found 298.1561 (± 0.0008) u, calculated 298.1569 u for $C_{19}H_{22}O_3$.

2,4-Diphenyl-1,5-dihydroxy-3-pentanone

Colorless needles, diastereomeric mixture; mp 85–86 °C; ^{1}H NMR δ 3.66–3.75 (4H, m), 4.09–4.31 (4H, m), 6.91–7.13 (10H, m); ^{13}C NMR δ 61.70, 64.73, 127.48, 128.57, 128.76, 129.33, 129.60, 134.94, 211.28; UV (CH_3CN) λ_{max} (nm) 259 (0.13), 297 (0.10); EIMS m/z (%) 270.1 ($M^{\bullet+}$, 0.20), 240 (10), 121 (52), 105 (5), 104 (100), 103 (27), 91 (10); HRMS: found 270.1264 (± 0.0008) u, calculated 270.1256 u for $C_{17}H_{18}O_3$.

To prepare the mesylate derivatives, the alcohols (2.5 mmol) were dissolved in a mixture of pyridine (25 mmol) and CH_2Cl_2 (3.5 mL). When cooled to 0 °C, methanesulfonyl chloride (10 mmol) diluted in CH_2Cl_2 (2 mL) was added dropwise to the reaction mixture with continuous stirring. Progress was monitored by NMR spectroscopy and reaction times ranged between 2.5–6.5 hours. The reaction was quenched with the addition of ice water and the mesylate product extracted using CH_2Cl_2. The organic layer was washed twice with 5% aqueous H_2SO_4, twice with saturated aqueous $NaHCO_3$, and twice with ice water. The organic fractions were combined and dried with $MgSO_4$, filtered and the solvent evaporated under reduced pressure. The crude product was purified using flash column chromatography on silica gel and eluted with ethyl acetate–hexane solvent mixtures. Alternatively, repetitive cold recrystallizations in ethyl acetate–hexane mixtures were carried out to purify the crystalline mesylate products. Dimesylates were synthesized similarly using the corresponding diols in a 1 : 8 : 20 molar ratio of diol–methanesulfonyl chloride–pyridine. All compounds were stored in the dark at 0 °C.

2-(4-Chlorophenyl)-3-oxobutyl methanesulfonate (2a)

$C_{11}H_{13}O_4SCl$; clear oil; ^{1}H NMR δ 2.14 (3H, s, CH_3), 2.98 (3H, s, SCH_3), 4.10–4.76 (3H, m, CH and CH_2), 7.15–7.38 (4H, m); ^{13}C NMR δ 29.48 (CH_3), 37.24 (SCH_3), 57.25 (CH), 69.17 (CH_2), 129.77, 129.86, 132.02, 134.82, 204.55 (CO); UV (CH_3CN) λ_{max} (nm) 267.0.

2,4-Diphenyl-3-oxopentyl 1,5-dimethanesulfonate (2b)

$C_{19}H_{22}O_7S_2$; fine white crystals; mp 114–116 °C; ^{1}H NMR δ 2.99 (6H, s), 4.23–4.33 (4H, m), 4.73–4.82 (2H, m), 6.88–7.14 (10H, m); ^{13}C NMR δ 37.42 (CH_3), 57.91 (CH), 69.58, 128.42, 128.65, 128.98, 132.40, 205.13 (CO); UV (CH_3CN) λ_{max} (nm) 253.0 (0.38), 293.0 (0.19); EIMS m/z (%) M^+ not observed, 234 (100), 205 (43), 128 (31), 104 (54), 103 (31), 91 (45).

2-(4-Fluorophenyl)-3-oxobutyl methanesulfonate (2c)

$C_{11}H_{13}FO_4S$; clear yellow oil; ^{1}H NMR δ 2.14 (3H, s, CH_3), 2.98 (3H, s, CH_3), 4.12–4.31 (2H, m), 4.70–4.78 (1H, dd, J = 8.54, 9.76 Hz), 7.03–7.33 (4H, m); ^{13}C NMR δ 29.27 (CH_3), 36.99 (SCH_3), 56.86 (CH), 69.33 (CH_2), 116.23, 116.57, 129.36, 129.41, 130.14, 130.27, 160.71, 164.65, 204.81 (CO); UV (CH_3CN) λ_{max} (nm) 263 (0.538), 269 (0.471); EIMS m/z (%) 165.1 (1.24), 123.0 (19.07), 122.0 (100.00), 121.0 (17.14), 109.1 (10.57), 101.1 (9.09), 42.0 (49.93); HRMS: found 165.0709 (± 0.0008) u, calculated 165.0716 u for $C_{10}H_{10}OF$.

2,4-Bis(4-methylphenyl)-3-oxopentyl 1,5-dimethanesulfonate (2d)

$C_{21}H_{26}O_7S_2$; white powder; mp 91–92 °C; ^{1}H NMR δ 2.25 and 2.36 (6H, two *singlets* with ratio 16 : 84, Ar–CH_3), 2.82 and 2.99 (6H, two *singlets*, 16 : 84, SCH_3), 4.00–4.80 (6H, *m*), 6.76–6.95 and 7.03–7.22 (8H, AA′BB′, two sets of aromatics with ratio 16 : 84); ^{13}C NMR δ 21.28 (CH_3), 37.24 (SCH_3), 55.09 (CH), 68.81 (CH_2), 128.74, 129.44, 129.66, 130.53, 139.11, 203.15 (CO); UV (CH_3CN) λ_{max} (nm) 263.9 (0.307), 292.7 (0.188).

2-(4-Methoxyphenyl)-3-oxobutyl methanesulfonate (2e)

$C_{12}H_{16}O_5S$; clear oil; ^{1}H NMR δ 2.12 (3H, s, CH_3), 2.97 (3H, s, SCH_3), 3.80 (3H, s, OCH_3), 4.06–4.76 (3H, m, CH and CH_2), 6.88–7.15 (4H, AA′BB′); ^{13}C NMR δ 29.25 (CH_3), 37.07

(SCH_3), 52.59 or 55.35 (OCH_3), 56.97 (CH), 69.60 (CH_2), 114.88, 125.30, 129.61, 159.80, 205.21 (CO); UV (CH_3CN) λ_{max} (nm) 273.0 (1.718), with shoulder at 279.0 (1.537); EIMS *m*/*z* (%) M^+ not observed, 150 (61), 135 (43), 134 (100), 133 (75), 121 (95), 119 (48), 79 (27), 77 (42).

Laser flash photolysis

The nanosecond laser flash photolysis system at Dalhousie University is of standard design and has been previously described.[29] The samples, typically 1 mL, were contained in 7 × 7 mm² laser cells made out of Suprasil quartz tubing and bubbled with a slow stream of dry nitrogen for 10 minutes prior to laser irradiation. The excitation source was the fourth harmonic from a Spectra Physics Nd:YAG GRC-100 laser (266 nm; ≤8 ns/pulse; ≤20 mJ/pulse). Transient signals from a monochromator/photomultiplier system were initially captured by a Tektronix 620A digital oscilloscope and transferred to a Power Macintosh computer for storage and processing. The laser system was computer controlled using the Power Macintosh and software written using the Labview programming language. The absorbance of the substrates at 266 nm was ≈ 0.3–0.4 in the 7 × 7 mm² laser cells. All experiments were carried out at room temperature (22 ± 1 °C).

Acknowledgements

F. L. C. gratefully acknowledges the Natural Science and Engineering Research Council of Canada (NSERC) for financial support of this research. S. F. L. thanks NSERC and the Izaak Walton Killam Memorial Foundation for postgraduate scholarships.

References

1 P. A. Frey, *Chem. Rev.*, 1990, **90**, 1343.
2 M. Fontecave, *CMLS, Cell. Mol. Life Sci.*, 1998, **54**, 684.
3 J. Stubbe, *Biochemistry*, 1988, **27**, 3893.
4 J. Stubbe, *Annu. Rev. Biochem.*, 1989, **58**, 257.
5 J. Stubbe and W. A. van der Donk, *Chem. Rev.*, 1998, **98**, 705.
6 These kinds of radicals also have utility outside of biological systems, especially as intermediates in synthetic chemistry. See for example: D. Crich and K. Ranganathan, *J. Am. Chem. Soc.*, 2002, **124**, 12422.
7 J. Retey, in *Stereochemistry*, ed. C. Tamm, Elsevier, Amsterdam, 1982.
8 B. T. Golding, in *B12*, ed. D. Dolphin, Wiley, New York, 1982, ch. 15.
9 R. G. Finke, D. A. Schiraldi and B. J. Mayer, *Coord. Chem. Rev.*, 1984, **54**, 1.
10 H. Halpern, *Science*, 1985, **227**, 869.
11 P. George, P. E. M. Siegbahn, J. P. Glusker and C. W. Bock, *J. Phys. Chem. B*, 1999, **103**, 7531.
12 D. M. Smith, B. T. Golding and L. Radom, *J. Am. Chem. Soc.*, 2001, **123**, 1664.
13 K. Warncke, J. C. Schmidt and S.-C. Ke, *J. Am. Chem. Soc.*, 1999, **121**, 10522.
14 J. Stubbe, *J. Biol. Chem.*, 1990, **265**, 5329.
15 J. Stubbe and W. A. van der Donk, *Chem. Biol.*, 1995, **2**, 793.
16 B.-M. Sjoberg, in *Nucleic Acids and Molecular Biology*, ed. F. Eckstein and D. M. J. Lilley, Springer, Berlin, 1995.
17 P. E. M. Siegbahn, *J. Am. Chem. Soc.*, 1998, **120**, 8417.
18 R. Lenz and B. Giese, *J. Am. Chem. Soc.*, 1997, **119**, 2784.
19 B. Giese, X. Beyrich-Graf, J. Burger, C. Kesselheim, M. Senn and T. Schaefer, *Angew. Chem., Int. Ed. Engl.*, 1993, **32**, 1742.
20 D. Schulte-Frohlinde and C. von Sonntag, in *Ionizing Radiation Damage to DNA*, ed. S. S. Wallace and R. B. Painter, Wiley-Liss, Inc., New York, 1990.
21 G. Koltzenburg, G. Behrens and D. Schulte-Frohlinde, *J. Am. Chem. Soc.*, 1982, **104**, 7311.
22 G. Behrens, G. Koltzenburg and D. Schulte-Frohlinde, *Z. Naturforsch., C: J. Biosci.*, 1982, **37**, 1205.
23 S. Steenken, *Chem. Rev.*, 1989, **89**, 503.
24 C. von Sonntag, *The Chemical Basis of Radiation Biology*, Taylor & Francis, London, 1987.
25 S. M. Hecht, *Bionconjugate Chem.*, 1994, **5**, 513.
26 W. K. Pogozelski and T. D. Tullius, *Chem. Rev.*, 1998, **98**, 1089.
27 D. Crich and X.-S. Mo, *J. Am. Chem. Soc.*, 1997, **119**, 249.
28 D. Crich and X.-S. Mo, *Tetrahedron Lett.*, 1997, **38**, 8169.
29 F. L. Cozens, M. O'Neill, R. Bogdanova and N. P. Schepp, *J. Am. Chem. Soc.*, 1997, **119**, 10652.
30 Substituents effects on the kinetics for the rearrangement of β-substituted radicals have previously been observed: (*a*) A. L. J. Beckwith and P. J. Duggan, *J. Am. Chem. Soc.*, 1996, **118**, 12838; (*b*) D. Crich and X.-Y. Jiao, *J. Am. Chem. Soc.*, 1996, **118**, 6666.
31 E. Taxil, L. Bagnol, J. H. Horner and M. Newcomb, *Org. Lett.*, 2003, **5**, 827.
32 D. Crich and G. F. Filzen, *Tetrahedron Lett.*, 1993, **34**, 3225.
33 K. Tokumura, T. Ozaki, H. Nosaka, Y. Saigusa and M. Itoh, *J. Am. Chem. Soc.*, 1991, **113**, 4974.
34 N. J. Turro, I. R. Gould and B. H. Baretz, *J. Phys. Chem.*, 1983, **87**, 531.
35 X. Zhang and W. M. Nau, *J. Phys. Org. Chem.*, 2000, **13**, 634.
36 L. J. Johnston and N. P. Schepp, *J. Am. Chem. Soc.*, 1993, **115**, 6564.
37 D. N. Nevill and H. J. Ren, *J. Org. Chem.*, 1989, **54**, 565.
38 R. M. O'Ferrall and S. I. Miller, *J. Am. Chem. Soc.*, 1963, **85**, 2440.
39 T. W. Bentley, M. Christl, R. Kemmer, G. Llewellyn and J. E. Oakley, *J. Chem. Soc., Perkin Trans. 2*, 1994, 2531.
40 X. Creary and C. Geiger, *J. Am. Chem. Soc.*, 1820, **104**, 4151.
41 K.-T. Liu, Y.-F. Duann and S.-J. Hou, *J. Chem. Soc., Perkin Trans. 2*, 1998, 2181.
42 N. J. Turro and G. C. Weed, *J. Am. Chem. Soc.*, 1983, **105**, 1861.